CHAPTER II

FREQUENCY RECONFIGURABLE PLANAR SLOT ANTENNA USING PIN DIODES

2.1 Introduction

Frequency reconfigurable antenna (FRA) as an alternative to multiple antennas and multiband antennas has become more profound as it increases the functionality of wireless platforms and improves their quality of service [2-7]. Minimal space requirements of FRA is an added advantage, especially where the form factors of the devices are small [8-11]. A good out-of-band noise rejection greatly reduces filtering requirements on a narrow-band reconfigurable antenna design [12-16].

The operating frequency of FRA can be reconfigured by controlling the effective length of the antenna structure. Slot cut into the patches can effectively provide a larger reconfiguration range without much increase in the physical dimension of the antenna [17-21]. Simply altering the slot configurations using electrical switches, the effective length of the antenna can be changed and thus, the resonating frequency.

In this chapter a meandered slot geometry based antenna with a switchable operating band is proposed. The design uses the advantage of the meandered slot to accommodate a lower resonant frequency with a relatively smaller patch. The desired adaptability is achieved by changing slot configuration through PIN diodes. The objective is to demonstrate multiple reconfigurations of antenna frequency using a fewer number of switching elements and with stable radiation characteristics. The simplicity of the reconfiguring circuitry is also taken into consideration. Before fabricating, the slotted antenna dimensions are optimized. A proof-of-concept design using metallic strips for ideal switches is carried out to achieve the desired performance. Reconfiguration mechanism (PIN diode) with its peripheral components like biasing lines, rf and dc blocks etc. are implemented and its functionality tested for different switching combinations.

The performance is determined by measuring the S11 parameter and radiation pattern. A short description of the measuring and simulation tools are mentioned before describing the design aspects for frequency reconfigurable antenna.

2.2 Measurement and simulation tools

The assessments of the developed antennas and reconfiguration techniques during the course of the work are carried out using the following tools.

S11 parameter measurement

S11 measurements are carried out using Agilent E8362C, PNA series vector network analyzer (VNA). Calibration of the VNA is carried out using Agilent 85052 D calibration kit. The antenna is connected to one of the calibrated port and frequency is swept from 6.0 to 9.0 GHz.

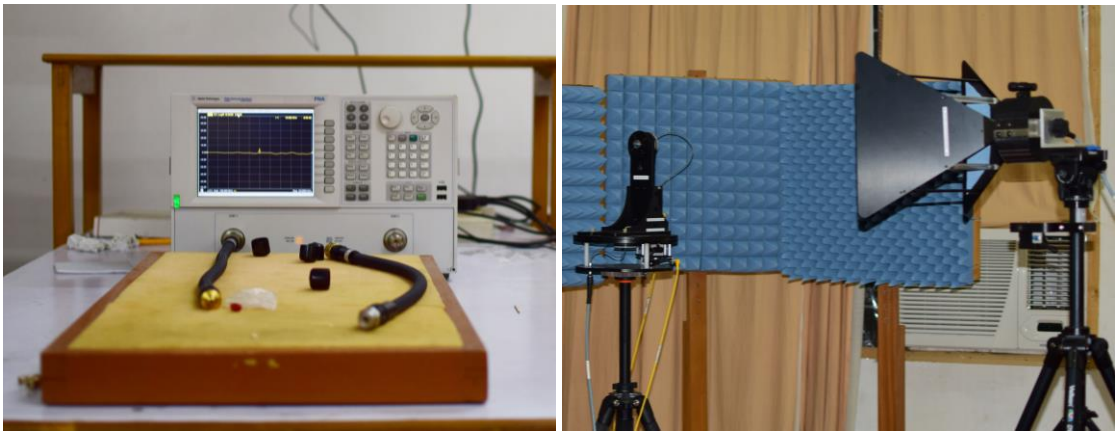

(a) (b)

Figure 2.1 (a) Agilent VNA and (b) Antenna Measurement System showing the reference horn antenna and automated turn table for the test antenna mounting

Radiation pattern measurement

The radiation pattern of the fabricated antenna is measured using an automated Antenna Measurement System from Diamond Engineering U.S.A and Agilent VNA. Measurements are taken with respect to a reference horn antenna (Gain 15 dBi) placed 1.5 meter apart from the antenna under test in the free space environment. The measured data are fed into the DAMS Antenna Measurement Studio for calculation of antenna parameters viz., beam angle, beam-width, directivity, gain etc. Parameters can also be obtained using equations given in [24].

Simulation software

All the works presented in this thesis are studied using CST Microwave Studio.

2.3 Rectangular microstrip patch geometry

The proposed meandered slot antenna is a modified form of a rectangular microstrip patch antenna (RMA). The conventional RMA geometry is chosen for developing the frequency reconfigurable antenna, as its design and performance parameters are well established. This makes the transformation easier and the performance of the developed antenna can easily be compared taking the standard RMA as the reference. Additionally, the RMA has an average gain of around 5 dBi – 9 dBi, which is considered as sufficient for handheld operations. The bandwidth of a typical microstrip patch antenna is around 4 % and considered as narrowband. However, a narrow band antenna with discrete frequency switching can be a suitable replacement to wideband antenna with sophisticated filters.

2.3.1 Base antenna design

The base antenna is designed to resonate at 8.00 GHz, on a glass epoxy (FR4, ε=4.3) substrate of thickness 1.6 mm, using a transmission line model (TLM) [24]. The schematic of the edge-fed RMA is shown in Figure 2.2. The length, L and width, W of the patch is determined using TLM technique by following equations [24]. The calculated L and W values are given in Table 2.1.

$$W = \frac{c}{2f_r}\sqrt{\frac{2}{\varepsilon_r + 1}} \tag{2.1}$$

$$\varepsilon_{reff} = \frac{\varepsilon_r + 1}{2} + \frac{\varepsilon_r - 1}{2}\left[1 + 12\frac{h}{W}\right]^{-1/2} \tag{2.2}$$

$$\Delta L = h \times 0.412\frac{(\varepsilon_{reff} + 0.3)\left(\frac{W}{h} + 0.264\right)}{(\varepsilon_{reff} - 0.258)\left(\frac{W}{h} + 0.8\right)} \tag{2.3}$$

$$L = \frac{c}{2f_r\sqrt{\varepsilon_{reff}}} - 2\Delta L \tag{2.4}$$

$$L_{eff} = L + 2\Delta L \tag{2.5}$$

where,

h = height of the substrate

ΔL = effective extension of length of the patch due to fringing fields

L_{eff} = effective length of the patch

ε_{reff} = effective dielectric constant

f_r = resonant frequency

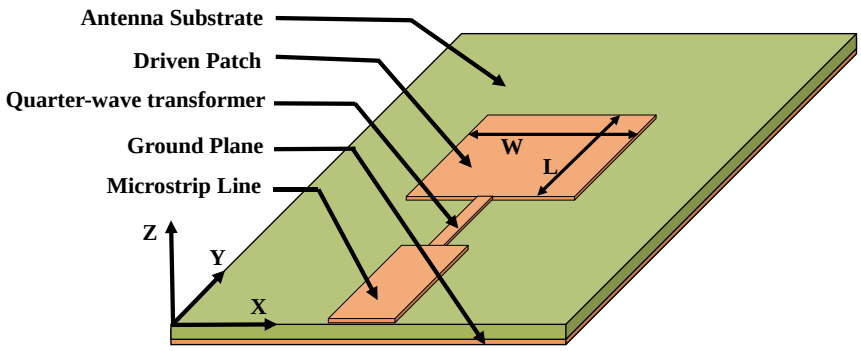

Figure 2.2 Schematic representation of a rectangular patch antenna

Table 2.1 Design specifications of the base antenna

Resonance Frequency (GHz)	Substrate Thickness (mm)	Permittivity (ε)	Length L (mm)	Width W (mm)
8.00	1.6	4.30	8.38	11.52

2.3.2 Performance studies of the base antenna

Performance of the basic rectangular patch antenna is studied by measuring and simulating the S11 parameter and radiation characteristics.

S11 parameter measurement

The measured and simulated S11 plots for the designed antenna is shown in Figure 2.3. The simulated and measured resonant frequencies are almost the same with a return loss of -26.04 dB and -32.96 dB, respectively.

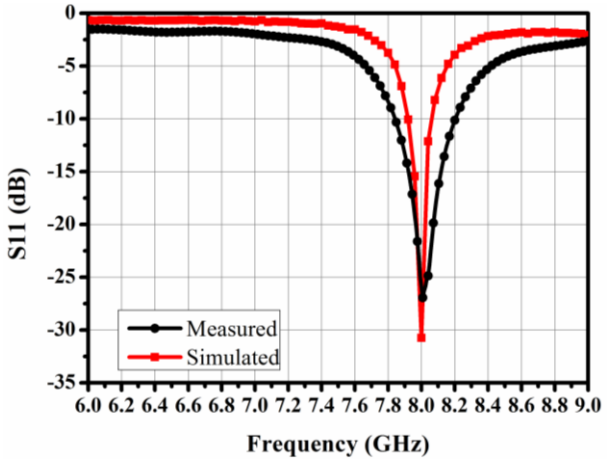

Figure 2.3 Measured and simulated S11 plots for fabricated RMA

Radiation pattern measurement

The base antenna is also studied for radiation characteristics. Measured and simulated co/cross-polar radiation patterns for both XZ and YZ planes are shown

in Figure 2.4. The patterns are broadside in nature with 0˚ beam direction and beam width of around 80.00˚ in both planes. The antenna has a measured directivity of 6.80 dB and gain 4.76 dBi. Measured and simulated parameters of the base antenna are listed in Table 2.2. The efficiency is around ~ 70 %.

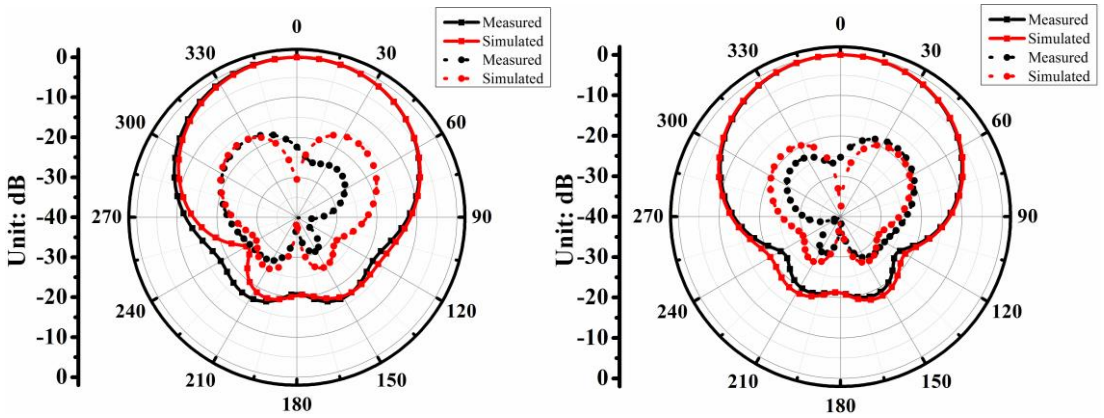

Figure 2.4 Measured and simulated radiation patterns of RMA fabricated on FR4 substrate (a) XZ plane, (b) YZ plane. Solid black and red line shows measured and simulated co-polar plots. Dotted black and red lines shows the corresponding cross-polar plots.

Table 2.2 Measured and simulated parameters of the base antenna

Frequency (GHz)		Bandwidth (MHz)		Directivity (dB)		Gain (dBi)	
Meas.	**Simul.**	**Meas.**	**Simul.**	**Meas.**	**Simul.**	**Meas.**	**Simul.**
8.00	8.04	400	250	6.80	6.98	4.76	4.88

Meas. = Measured Simul. = Simulated

2.4 Frequency reconfigurable meandered slot antenna

The designed rectangular patch antenna is converted into a frequency reconfigurable antenna. At first, meandered slots are introduced to the patch structure and then necessary modifications required for the reconfiguration are carried out.

2.4.1 Design of the meandered slot antenna

The antenna patch geometry is modified by incorporating two non-identical cross-shaped meandered slots in the middle of the non-radiating edges (NREs) of a standard RMA (Figure 2.5). Cross-shaped slot used which is similar to a self-repeating structure, when incorporated in the NRE of the rectangular patch takes

the form of a second-order quasi Minkowski curve [27, 28]. The meandered nature of the curve pushes the patch boundary inside, showing a trend to fill the area within. This eventually extends the length of the NRE into the interiors of the patch without increasing the overall antenna dimension. This eventually elongates the surface current paths resulting in a lowering of frequency from the designed value of 8.00 GHz.

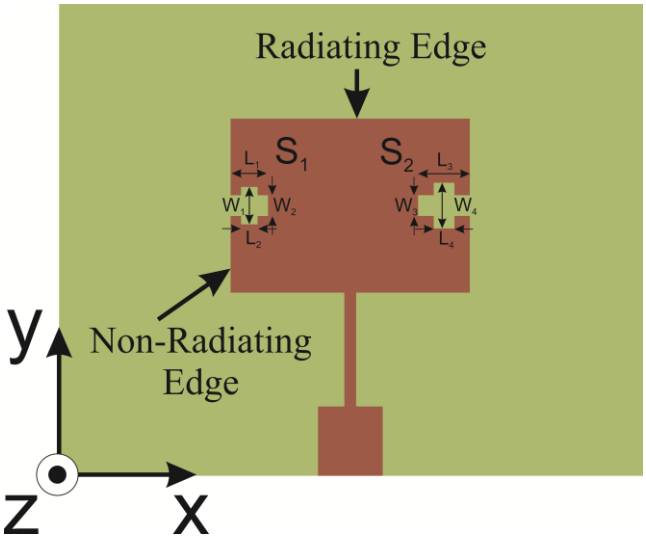

Figure 2.5 Schematic diagram of the meandered slot microstrip patch antenna

2.4.2 Optimization of the slot dimensions

Precise slot dimensions are optimized (using CST MW Studio) for a gradual shift of individual band positions, maintaining a continuous return loss of – 10 dB range. Optimization is carried out in three steps as shown in Figure 2.6. Firstly, cross slot, S_1, is inserted into one of the non-radiating edge (NRE) of the simulated structure, while keeping the other NRE unmodified. The dimension (W_1, L_1, W_2 and L_2) of slot S_1 is so selected that the resonating frequency of the patch shifts to the lower side of the base RMA resonating at 8.0 GHz. Initially, W_1 and L_1 are arbitrarily taken as 2.00 mm and W_2 and L_2 are as 1.00 mm. Optimization of the slot parameters is carried out to maintain a cascaded behaviour at – 10 dB level, while shifting the resonating frequency. In the next step slot S_2, of slightly larger dimension (W_3, L_3, W_4 and L_4 of 2.00 mm) than S_1 is inserted on the other edge while keeping the opposite edge unmodified. The dimension of slot S_2 is optimized to have – 10 dB bandwidth consistency to the previous structure (Figure 2.6 (b)).

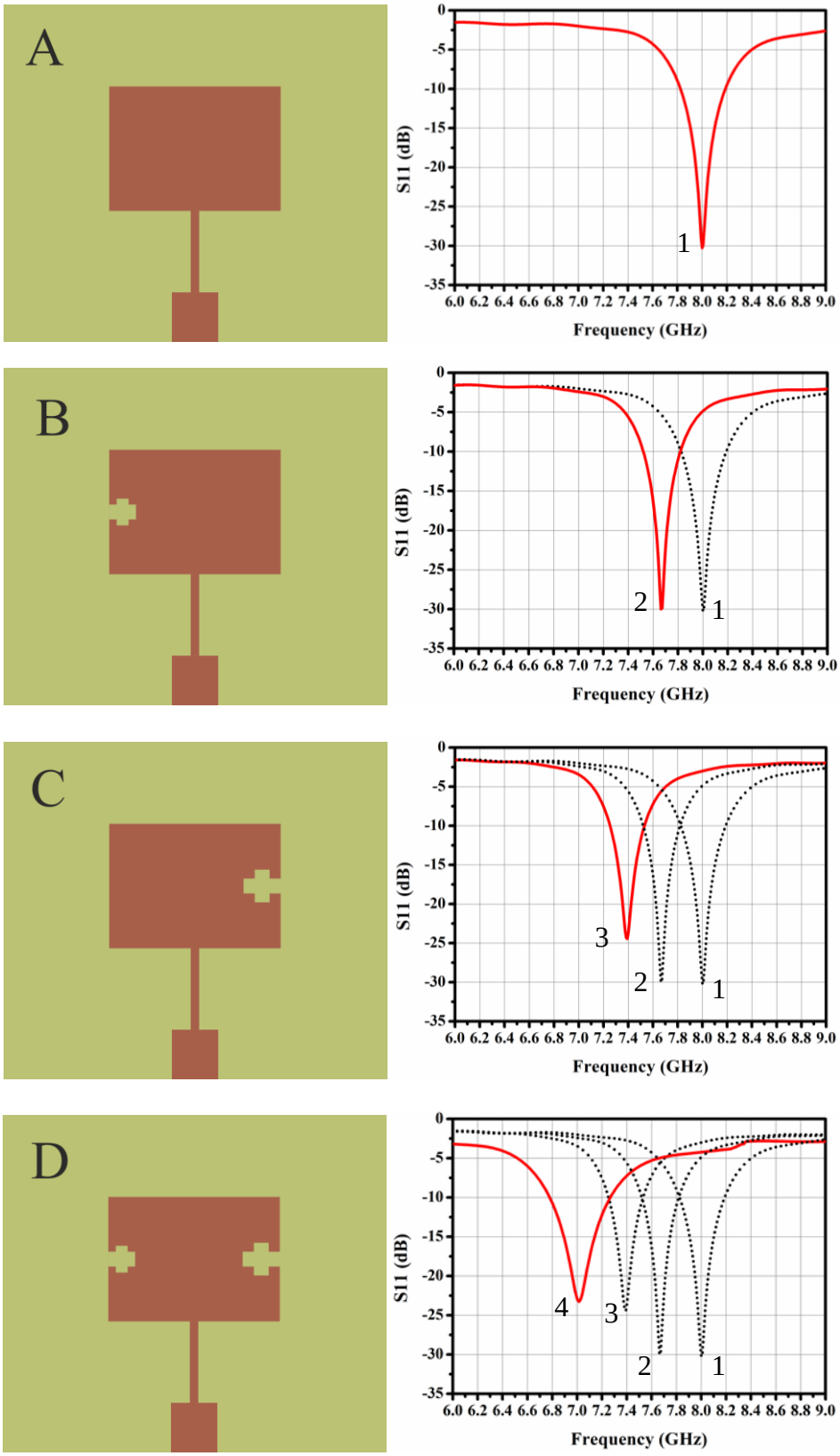

Figure 2.6 Schematic diagram of slot optimization process and corresponding S11 plots. Solid lines shows the S11 parameters of present configuration while dotted lines shows the previous configurations.

Finally, both the slots S_1 and S_2 are incorporated into the patch, which leads to further lowering of the resonant frequency. The slots dimension are further fine-tuned by varying its lengths and widths to ensure successive frequency shifting for all these steps and a continuum -10dB bandwidth. The optimized dimension of each slot is listed in Table 2.3. In Figure 2.6 (a) schematic of the unmodified patch antenna and the corresponding S11 with a resonating notch at 8.00 GHz are shown. Figure 2.6 (b) shows the optimized slot S_1 and the related S11 value in solid red line. The dotted line presented in the plot marks the S11 of the unmodified antenna. Slot S_2 is incorporated and the resulting frequency plot (solid red line) are given in Figure 2.6 (c). Similar to the previous case (Figure 2.6 (b)) the two dotted line plots shows the position of the resonating frequency of the base antenna and the antenna with only slot S_1. Figure 2.6 (d) depicts the meandered slot antenna with slots S_1 and S_2 and the corresponding plot with solid red line shows the resonating frequency. The dotted lines gives the positions of the antenna frequency for all the previous configurations. Both the slots S_1 and S_2 are positioned at the center of the non – radiating edge.

Table 2.3 Optimized slot dimensions of the modified patch antenna

Slot S_1	L_1=1.80 mm	L_2=0.80 mm	W_1=1.80 mm	W_2=1.00 mm
Slot S_2	L_3=2.50 mm	L_4=1.00 mm	W_3=1.00 mm	W_4=2.20 mm

The narrow bandwidth of the individual resonating notch limits the maximum range over which frequency can be shifted in a cascaded manner. Further increase of slot dimension (beyond the optimized value), the resonating frequency do shift to lower values but the -10 dB continuum is not maintained.

2.4.3 Proof of concept of reconfiguration

From the simulation study as shown in Figure 2.6, it is found that with the inclusion of slots in the order No Slot – Slot S1 – Slot S2 – Slots S1 and S2, the resonating frequency is gradually shifted. Similarly, recapturing of the original frequency is also possible through the reversion of the order of slot insertions.

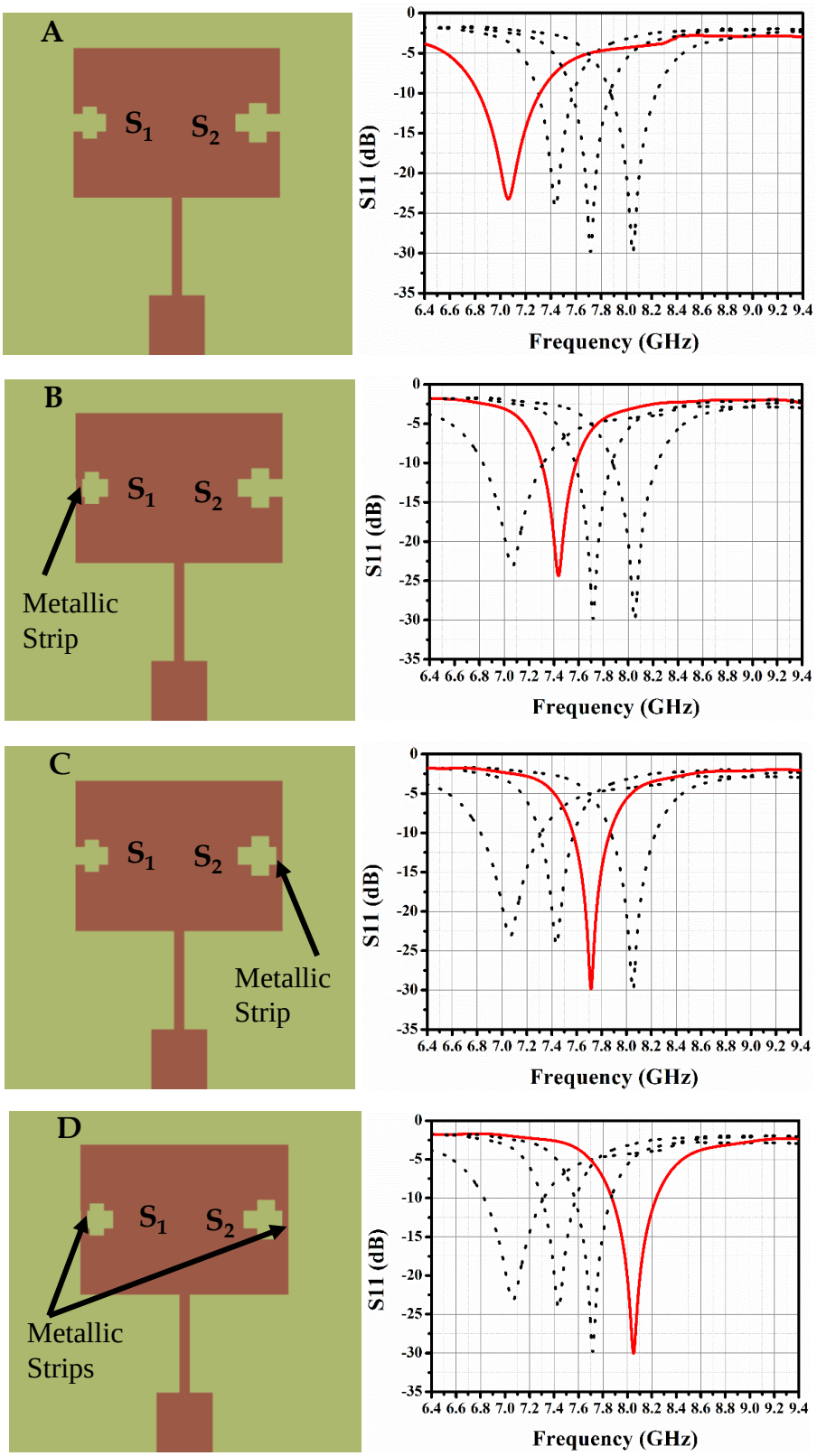

Figure 2.7 Schematics illustrating the simulated frequency reconfiguration with corresponding plots. The dotted line represent all the accessible frequency bands and the solid red line represents the frequency of the corresponding configuration.

For a proof-of-concept design, a shorting strip at the open end of each slot is placed. The strip bypasses a major part of the current flowing at the slot boundary and reduces the effective length of the patch, which was elongated by the slots. This shifts the frequency to a higher value. Upon the removal of the shorting strips the effective length is again extended and the resonating frequency is bounce back to the original value. Since, each step as shown in Figure 2.6 corresponds to a particular frequency value, each of these frequencies can be acquired by simply activating the related slot.

Figure 2.7 (a) shows an RMA with both the slots S_1 and S_2 inserted to the non-radiating edges. S11 plots of the antenna show a resonating notch at 7.00 GHz indicated by a red colored solid line. The black dotted line marks the other accessible frequency values. In Figure 2.7 (b) a shorting strip is placed at the open end of slot S_1. The corresponding S11 plot reveals a shift in the frequency (red solid line). Similarly, slot S_2 is shorted while keeping slot S_1 open and the resulted frequency shift is shown in the S11 plot. Finally, both slot S_1 and S_2 are shorted and the antenna resonates at around 7.90 GHz, which is closer to the design frequency (8.00 GHz) of the base RMA.

2.5 Implementation and study of reconfiguration mechanism

The real-time alteration of the path length is realized by using an electrically switchable shorting strip. Details of the switching mechanism and the performance study are described in the following sections.

2.5.1 Reconfigurable meandered slot antenna with PIN diode

The proposed reconfiguration technique uses PIN diodes as switching elements. Two PIN diodes (NXP Semiconductors BAP 70-02) are placed at the slots' open end, through two separate biasing networks at the peripheral, as shown in Figure 2.8 (a). Each of the biasing networks contains two capacitors of 1.0 pF as dc blocks, two inductors (2.0 nH) as rf isolators. Both the networks are powered by a 5 volts regulated supply. The lumped elements used in the proposed work are selected based on the information provided by the manufacturers in their

respective datasheets (Attached as Appendix). PIN diodes are simulated as an R – L – C series circuit to get an idea about their RF performance. The circuits are modelled as the equivalent circuit of the PIN diode in it's ON and OFF state. R, L and C values can be found in the datasheet of BAP 70-02. In ON mode, simulated insertion loss is around 0.2 dB for the range 1.00 GHz – 10.00 GHz and in OFF mode it is lower than – 20 dB. DC block capacitors (Johanson Technology: Series 0603) have series resonant frequency up to around 20.00 GHz and equivalent series

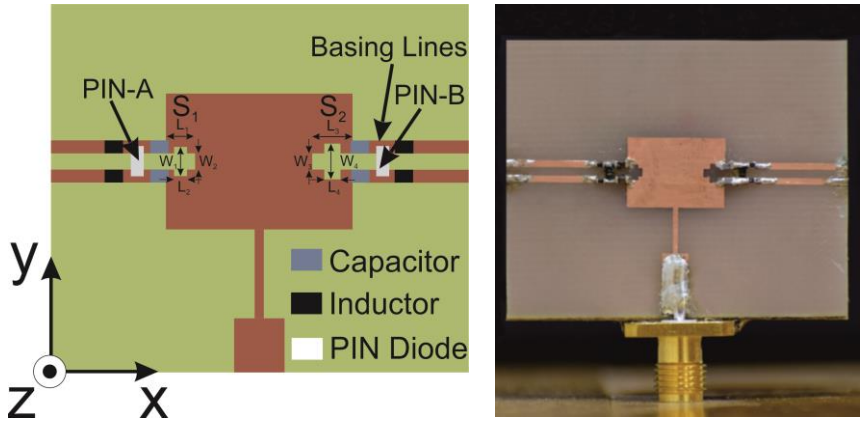

(a) (b)

Figure 2.8 Schematics of the (a) Designed antenna and (b) Fabricated antenna

resistance of about 160 mΩ. RF block inductors (Multicomp: Series 0402) have series resonant frequency at around 8.00 GHz and maximum dc resistance of 0.35 Ω. Both diodes can be separately set to either ON or OFF states by altering the biasing condition. When the diodes are OFF, the connection across the slot end vanishes contributing to a current path elongation along the slot dimension, thereby lowering the resonant frequency. ON state of the diode establishes a shorter path to the surface current and the frequency is shifted to a higher value.

2.5.2 Performance studies of the reconfigurable slot antenna

S11 parameters

The prototype is tested for experimental verification. The measured and simulated S11 parameters of the meandered slot antenna are shown in Figure 2.9. Initially, when both diodes are in OFF state, a resonating notch occurs at 6.80 GHz (Mode 1). In Mode 2 operation frequency is shifted to 7.34 GHz. Here PIN Diode-A is in

ON state, i.e. slot S_1 is shorted. In Mode, 3 operation PIN Diode-B attached to Slot S2 is in ON state and this shifts the resonating frequency to 7.80 GHz. Finally, with both the diodes in ON state, the antenna resonates at 8.19 GHz.

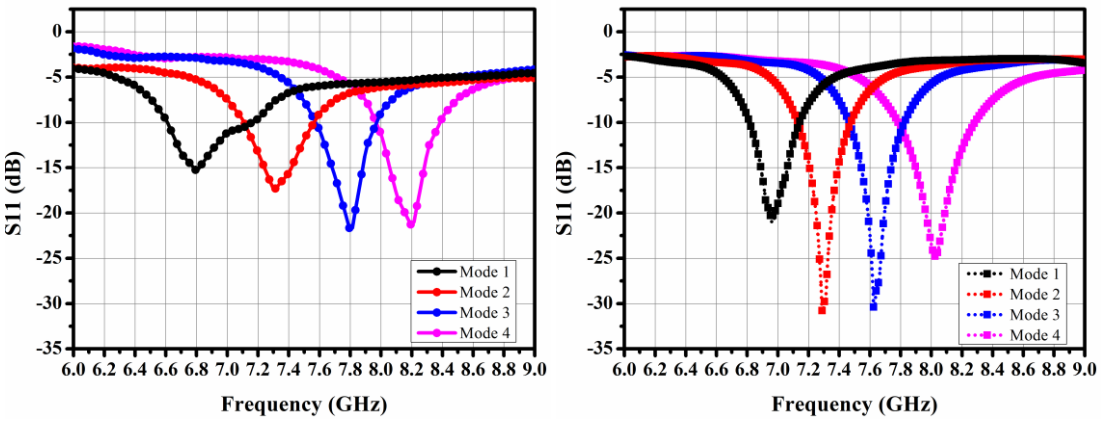

Figure 2.9 (a) Measured and (b) Simulated S11 parameters

Different PIN diode states for all the modes and corresponding frequencies are given in Table 2.4. From the measured results it is observed that the proposed antenna offers a single operating band which can be set to four positions in the electromagnetic spectrum by altering the PIN diode's biasing conditions. It is also noted that precise selection of slot dimensions helps in hopping of frequency in a cascaded manner to cover a range of 1.80 GHz (6.6 GHz – 8.4 GHz).

Table 2.4 PIN diode states and corresponding frequencies with measured directivity and gain

Mode	PIN State		Frequency (GHz)		Directivity (dB)	Gain (dBi)	Efficiency (%)
	PIN A	PIN B	Measured	Simulated			
1	OFF	OFF	6.80	6.98	7.24	4.80	66.29
2	ON	OFF	7.34	7.30	7.09	4.98	70.24
3	OFF	ON	7.80	7.62	7.32	5.32	72.68
4	ON	ON	8.19	8.02	7.40	5.48	74.06

A -10 dB bandwidth is maintained throughout the range. Simulated results for S11 parameters are also in good agreement with the measured results. However, slight variations could be due to the effect of fabrication tolerances and presence of the peripheral network.

Surface current distribution study

As mentioned in the previous section, redistribution of surface current is the key to frequency reconfiguration in this approach and the idea can be validated from current distribution plots for different operating modes (Figure 2.10).

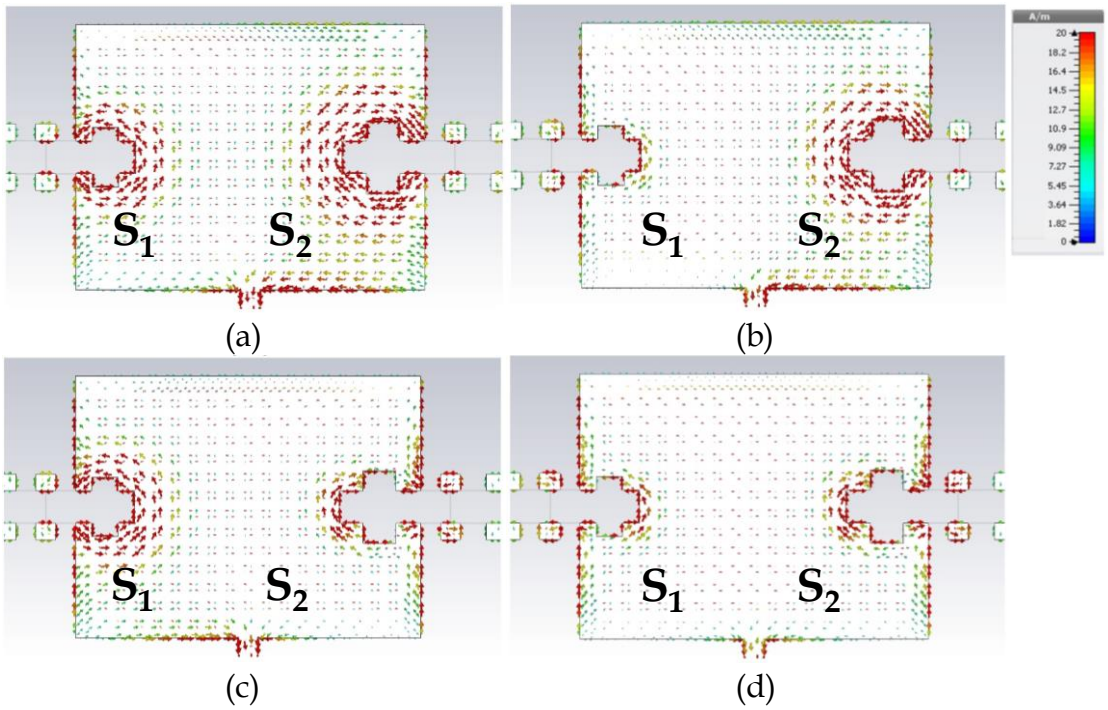

Figure 2.10 Surface current distribution: (a) Mode 1, (b) Mode 2, (c) Mode 3 and (d) Mode 4

It is observed that concentrations of current along the slot edges are larger for PIN diode in OFF state (Figure 2.10 (a)), while for PIN in ON state, current gets redistributed, due to the presence of shorting path across the slot end, indicated by a decrease in current concentration along the slot edges and simultaneous increased along the PIN network (Figure 2.10 (d)). In Figure 2.10 (b) and (c), only one PIN diode is alternatively set to ON mode. Figure 2.10 (b) depicts a decrease in current density across the perimeter of slot S_1 and in Figure 2.9 (c) across slot S_2.

Radiation pattern measurement

Figure 2.11 and Figure 2.12 shows normalized radiation patterns of the antenna for all possible modes. The designed antenna offers consistent radiation patterns at all the reconfigured frequencies. In XZ plane measured radiation pattern shows a

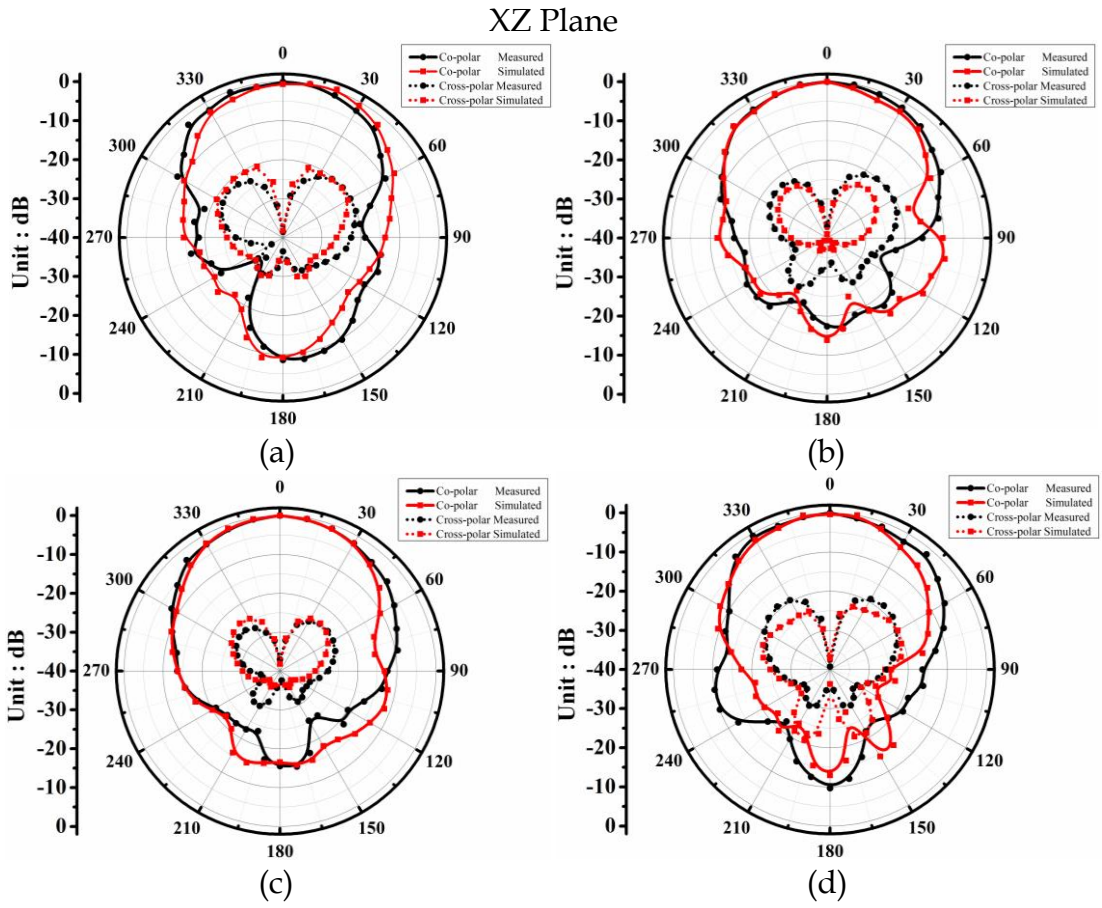

Figure 2.11 Measured and simulated radiation patterns in XZ plane (a) Mode 1, (b) Mode 2, (c) Mode 3 and (d) Mode 4. Solid black and red line shows measured and simulated co-polar plots. Dotted black and red lines shows the corresponding cross-polar plots.

fixed main lobe direction at 0° with an average – 3 dB beamwidth of about 74.89°. Similar consistencies are maintained in the YZ plane (Figure 2.12) also, giving an average beam width of 76.98° with the main lobes at around 4°. A low cross polarization level at each of the frequency is recorded. Simulated radiation patterns also show similar stability at all the switched frequencies. From the study, it could be said that the effect of biasing lines on the radiation patterns are very low as the measured patterns are almost identical to that of a standard RMA (Figure 2.4).

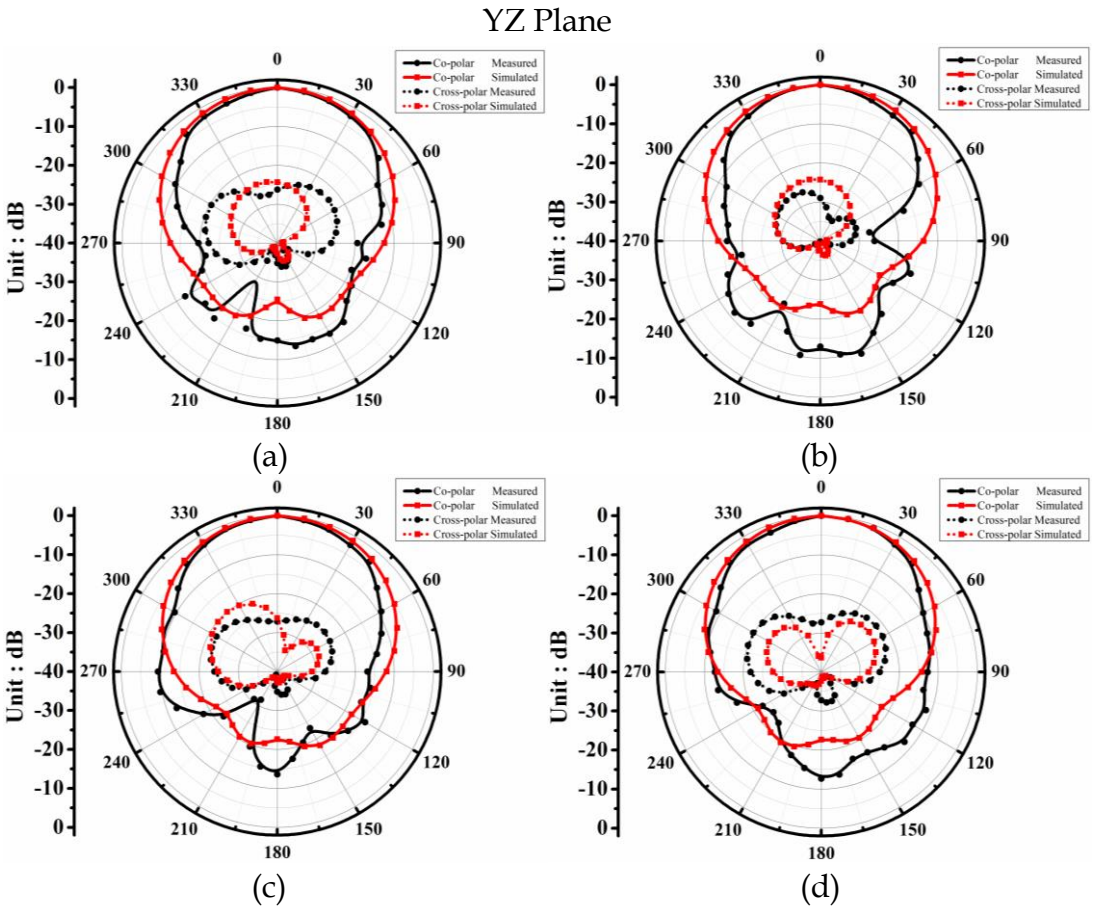

Figure 2.12 Measured and simulated radiation patterns in YZ plane (a) Mode 1, (b) Mode 2, (c) Mode 3 and (d) Mode 4. Solid black and red line shows measured and simulated co-polar plots. Dotted black and red lines shows the corresponding cross-polar plots.

Performances of the antenna in terms of directivity and gain are also tested and results indicate a fairly stable frequency reconfiguration. The measured directivities lie between 7.09 dB – 7.40 dB, while the measured average gain is about 5.14 dBi (4.80 dBi – 5.48 dBi). Directivity and gain of the antenna with corresponding frequencies are given in Table 2.4. The gain is found to decrease as the frequency shifts to the lower side, reasoned with an increase of input impedance mismatch with a shift in frequency. This limits the maximum attainable span of frequency. A gradual increase of input impedance mismatch is observed in the S11 plot shown in Figure 2.9, indicated by the increased reflection loss. A performance wise comparison of some relevant works is presented in Table 2.5. It is seen that in most of the listed planar reconfigurable antennas, the frequency coverage range and antenna gain are less than the proposed antenna.

Table 2.5 Comparison of the proposed antenna with previously reported recent work of frequency reconfigurable antenna

Ref. No.	Antenna Geometry	Switching Elements Types and Quantity		Max. Bias Volt. (V)	Frequency Range (GHz)		Radiation Pattern Consistency	Gain (dBi)
[1]	Planar, U-Slot	Varactor	2	14	1.07 (2.46 – 3.53)	Cont.	Yes	5.0 – 3.6
[22]	Planar	PIN	2	15	0.34 (2.55 – 2.89) 0.23 (4.51 – 4.74)	Scatt.	Yes	3 – 1
		Varactor	1		0.29 (1.96 – 2.25) 0.30 (3.91 – 4.21) 0.27 (1.59 – 1.86)			
[23]	Planar	PIN	4	5	1.00 (1.50 – 2.50)	Cont.	No	2.2 – 1.5
[9]	Planar	PIN	1	14	1.06 (0.42 – 1.48)	Cont.	Yes	Above -0.4
		Varactor	1					
[25]	Planar	PIN	5	5	4.60 (6.00 – 10.6)	Cont.	No	3.2 – 1.7
[26]	Non – Planar	Varactor	8	25	0.28 (0.76 – 1.04) 0.37 (1.50 – 1.87)	Scatt.	Yes	5.5 – -0.7
[29]	Planar	PIN	4	1.5	2.59 (1.55–4.14) 1.15 (2.13–3.28) 1.26 (3.24–4.50)	Cont.	Yes	3.3 – 1.8
[30]	Planar	PIN	2	5	0.31 (2.31–2.62) 0.19 (5.13–5.32)	Scatt.	Yes	3.0
Proposed	Planar	PIN	2	5	1.80 (6.60 – 8.40)	Cont.	Yes	5.4 – 4.8

Cont. = Continuous Scatt. = Scattered

In [25], a wide frequency coverage is reported; however, consistency of radiation patterns throughout the entire accessible range is not observed in the approach and in [29] gain is less than the proposed work.

2.6 Discussion

The presented approach offers a simple way of frequency reconfiguration without increasing the antenna's physical dimension. It is intended to keep the number of PIN diodes as low as possible to make the design simple and reduce the amount of losses introduced due to the lossy behavior of PIN diodes. Use of meandered slots to shift the operating frequency helps in achieving the desired frequency

agility without much compromising the consistency of the radiation pattern. The degree of shift is totally dependent on perturbation of surface current distribution and is controlled by the size of the slots. The inside insertion of cross-shaped meandered slots to the patch geometry, forces surface currents to travel a much longer path within a small area near non-radiating edges, resulting in minor variations in field distributions across the periphery of the patch which in turn generates almost identical radiation patterns for all the switching conditions.

The designed antenna can be reconfigured to four different positions by independently controlling each PIN diode over a continuous range of frequency. An accessible range of 1.8 GHz is achieved through four reconfigurable bands. In terms of radiation characteristics, it shows almost identical broadside radiation patterns with an average gain of 5.14 dBi. A consistent -10 dB bandwidth is maintained during the whole reconfigurable range. Slight degradations in the peak gain values observed towards the lower end of the operating range are mainly because of the increase in input impedance mismatch.

The proposed antenna could potentially be a suitable solution for hopping between closely spaced bands over a continuous range. Reduction in antenna patch dimension, low costing and simple reconfigurable circuitry are the other features of the designed antenna.

References

[1] Ren, Z., Li, W.-T., Xu, L., and Shi, X.-W. A compact frequency reconfigurable unequal U-slot antenna with a wide tunability range. *Progress In Electromagnetics Research Letters,* 39:9-16, 2013.

[2] Symeon, N., Bairavasubramanian, R., Lugo, C., Carrasquillo, I., Thompson, D.C., Ponchak, G.E., Papapolymerou, J., and Tentzeris, M.M. Pattern and frequency reconfigurable annular slot antenna using PIN diodes. *IEEE Transactions on Antennas and Propagation,* 54(2):439-448, 2006. DOI:10.1109/TAP.2005.863398

[3] Lim, J.H., Back, G.T., Ko, Y.I., Song, C.W., and Yun, T.Y. A Reconfigurable PIFA Using a Switchable PIN-Diode and a Fine-Tuning Varactor for USPCS/WCDMA/m-WiMAX/WLAN. *IEEE Transactions on Antennas and Propagation,* 58(7):2404-2411, 2010. DOI:10.1109/TAP.2010.2048849

[4] Panagamuwa, C.J., Chauraya, A., and Vardaxoglou, J. Frequency and beam reconfigurable antenna using photoconducting switches. *Antennas and Propagation, IEEE Transactions on,* 54(2):449-454, 2006.

[5] Christodoulou, C.G., Tawk, Y., Lane, S.A., and Erwin, S.R. Reconfigurable antennas for wireless and space applications. *Proceedings of the IEEE,* 100(7):2250-2261, 2012.

[6] Li, T., Zhai, H., Wang, X., Li, L., and Liang, C. Frequency-Reconfigurable Bow-Tie Antenna for Bluetooth, WiMAX, and WLAN Applications. *IEEE Antennas and Wireless Propagation Letters,* 14:171-174, 2015. DOI:10.1109/LAWP.2014.2359199

[7] Yang, S., Zhang, C., Pan, H.K., Fathy, A.E., and Nair, V.K. Frequency-reconfigurable antennas for multiradio wireless platforms. *IEEE Microwave Magazine,* 10(1):66-83, 2009. DOI:10.1109/MMM.2008.930677

[8] Majid, H.A., Rahim, M.K.A., Hamid, M.R., and Ismail, M.F. A Compact Frequency-Reconfigurable Narrowband Microstrip Slot Antenna. *IEEE*

Antennas and Wireless Propagation Letters, 11:616-619, 2012. DOI:10.1109/LAWP.2012.2202869

[9] Li, H., Xiong, J., Yu, Y., and He, S. A Simple Compact Reconfigurable Slot Antenna With a Very Wide Tuning Range. *IEEE Transactions on Antennas and Propagation,* 58(11):3725-3728, 2010. DOI:10.1109/TAP.2010.2071347

[10] Soltani, S., Lotfi, P., and Murch, R.D. A Port and Frequency Reconfigurable MIMO Slot Antenna for WLAN Applications. *IEEE Transactions on Antennas and Propagation,* 64(4):1209-1217, 2016. DOI:10.1109/TAP.2016.2522470

[11] Shynu, S., Augustin, G., Aanandan, C.K., Mohanan, P., and Vasudevan, K. Design of compact reconfigurable dual frequency microstrip antennas using varactor diodes. *Progress In Electromagnetics Research,* 60:197-205, 2006.

[12] Aberle, J.T., Sung-Hoon, O., Auckland, D.T., and Rogers, S.D. Reconfigurable antennas for wireless devices. *IEEE Antennas and Propagation Magazine,* 45(6):148-154, 2003. DOI:10.1109/MAP.2003.1282191

[13] Bhattacharjee, T., Jiang, H., and Behdad, N. A Fluidically Tunable, Dual-Band Patch Antenna With Closely Spaced Bands of Operation. *IEEE Antennas and Wireless Propagation Letters,* 15:118-121, 2016. DOI:10.1109/LAWP.2015.2432575

[14] Hinsz, L., and Braaten, B.D. A Frequency Reconfigurable Transmitter Antenna With Autonomous Switching Capabilities. *IEEE Transactions on Antennas and Propagation,* 62(7):3809-3813, 2014. DOI:10.1109/TAP.2014.2316298

[15] Nair, S.V.S., and Ammann, M.J. Reconfigurable Antenna With Elevation and Azimuth Beam Switching. *IEEE Antennas and Wireless Propagation Letters,* 9:367-370, 2010. DOI:10.1109/LAWP.2010.2049332

[16] Barrio, S.C.D., Pelosi, M., Pedersen, G.F., and Morris, A. Challenges for Frequency-Reconfigurable Antennas in Small Terminals. in *2012 IEEE Vehicular Technology Conference (VTC Fall)*, 1-5, 2012.

[17] Fan, Y., and Rahmat-Samii, Y. Patch antennas with switchable slots (PASS) in wireless communications: concepts, designs, and applications. *IEEE Antennas and Propagation Magazine,* 47(2):13-29, 2005. DOI:10.1109/MAP.2005.1487774

[18] Dey, S., and Mittra, R. Compact microstrip patch antenna. *Microwave and Optical Technology Letters,* 13(1):12-14, 1996.

[19] Lee, K.F., Luk, K.M., Tong, K.F., Shum, S.M., Huynh, T., and Lee, R.Q. Experimental and simulation studies of the coaxially fed U-slot rectangular patch antenna. *IEE Proceedings - Microwaves, Antennas and Propagation,* 144(5):354-358, 1997. DOI:10.1049/ip-map:19971334

[20] Weigand, S., Huff, G.H., Pan, K.H., and Bernhard, J.T. Analysis and design of broad-band single-layer rectangular U-slot microstrip patch antennas. *IEEE Transactions on Antennas and Propagation,* 51(3):457-468, 2003. DOI:10.1109/TAP.2003.809836

[21] Yang, F., Xue-Xia, Z., Xiaoning, Y., and Rahmat-Samii, Y. Wide-band E-shaped patch antennas for wireless communications. *IEEE Transactions on Antennas and Propagation,* 49(7):1094-1100, 2001. DOI:10.1109/8.933489

[22] Koley, S., and Mitra, D. A compact dual-band reconfigurable open-end slot antenna for cognitive radio front end system. *Progress In Electromagnetics Research C,* 58:33-41, 2015.

[23] Sharma, S., and Tripathi, C.C. Frequency reconfigurable U-slot antenna for SDR application. *Progress In Electromagnetics Research Letters,* 55:129-136, 2015.

[24] Balanis, C.A. *Antenna theory: analysis and design.* John Wiley & Sons. 2016.

[25] Pazin, L., and Leviatan, Y. Reconfigurable Slot Antenna for Switchable Multiband Operation in a Wide Frequency Range. *IEEE Antennas and Wireless Propagation Letters,* 12:329-332, 2013. DOI:10.1109/LAWP.2013.2246855

[26] Nguyen-Trong, N., Piotrowski, A., and Fumeaux, C. A Frequency-Reconfigurable Dual-Band Low-Profile Monopolar Antenna. *IEEE Transactions on Antennas and Propagation,* 65(7):3336-3343, 2017. DOI:10.1109/TAP.2017.2702664

[27] Oliveira, E.E.C., Silva, P.H.d.F., Campos, A.L.P.S., and d'Assunção, A.G. Small-size quasi-fractal patch antenna using the Minkowski curve. *Microwave and Optical Technology Letters,* 52(4):805-809, 2010. DOI:10.1002/mop.25071

[28] Agrawal, A.K., and Vinoy, K.J. Microstrip coupled line bandpass filter using quasi minkowski fractal shape for suppression of the second harmonic. in *2015 IEEE MTT-S International Microwave and RF Conference (IMaRC)*, 412-415, 2015.

[29] Choukiker, Y.K., and Behera, S.K. Wideband frequency reconfigurable Koch snowflake fractal antenna. *IET Microwaves, Antennas & Propagation,* 11(2):203-208, 2017.

[30] Ali, T., and Biradar, R.C. A compact hexagonal slot dual band frequency reconfigurable antenna for WLAN applications. *Microwave and Optical Technology Letters,* 59(4):958-964, 2017. DOI:doi:10.1002/mop.30443